



1 Merlivat et al, July 4, 2017.docx  
2 **Increase of dissolved inorganic carbon and decrease of pH in near surface**  
3 **waters of the Mediterranean Sea during the past two decades**

4

5

6 Liliane. Merlivat <sup>a</sup>, Jacqueline. Boutin <sup>a</sup>, David. Antoine <sup>b,c</sup>, Laurence. Beaumont <sup>d</sup>, Melek.  
7 Golbol <sup>b</sup>, Vincenzo. Vellucci. <sup>b</sup>

8

9 <sup>a</sup> Sorbonne Universités (UPMC, Univ Paris 06)-CNRS-IRD-MNHN, LOCEAN Laboratory,  
10 F-75005 Paris, France

11 <sup>b</sup> Sorbonne Universités (UPMC, Univ Paris 06)-CNRS, LOV, Observatoire Océanologique,  
12 Villefranche-sur-Mer 06230, France

13 <sup>c</sup> Remote Sensing and Satellite Research Group, Department of Physics and Astronomy,  
14 Curtin University, Perth, WA 6845, Australia

15 <sup>d</sup> Division Technique INSU-CNRS, 92195 Meudon Cedex, France

16

17 Corresponding author: L. Merlivat ([merlivat@locean.upmc.fr](mailto:merlivat@locean.upmc.fr))

18

19

20 **Abstract**

21 Two three-year-long time series of hourly measurements of the fugacity of CO<sub>2</sub> (fCO<sub>2</sub>) in the  
22 upper 10m of the surface layer of the northwestern Mediterranean Sea have been recorded by  
23 CARIOCA sensors almost two decades apart, in 1995-1997 and 2013-2015. By combining  
24 them with alkalinity derived from measured temperature and salinity, we calculated changes  
25 of pH and dissolved inorganic carbon (DIC). DIC increased in surface seawater by ~ 25 μmol  
26 kg<sup>-1</sup> and fCO<sub>2</sub> by 40 μatm, whereas seawater pH decreased by ~ 0.04 (0.0021 yr<sup>-1</sup>). The DIC  
27 increase is larger than expected from equilibrium with atmospheric CO<sub>2</sub>. This supports the  
28 hypothesis of a ~15% contribution of the Atlantic Ocean as a source of anthropogenic carbon  
29 to the Mediterranean Sea through the strait of Gibraltar. We estimate that the part of DIC  
30 accumulated over the last 18 years represents ~30% of the total change since the beginning of  
31 the industrial period.



32

33 **1 Introduction**

34 The concentration of atmospheric carbon dioxide (CO<sub>2</sub>) has been increasing rapidly over the  
35 20<sup>th</sup> century and, as a result, the concentration of dissolved inorganic carbon (DIC) in the near  
36 surface ocean increases, which drives a decrease in pH in order to maintain a chemical  
37 equilibrium [Millero, 2007]. These changes have complex direct and indirect impacts on  
38 marine organisms and ecosystems [Gattuso and Hansson, 2011]. Empirical methods to  
39 estimate the anthropogenic CO<sub>2</sub> penetration in the ocean since the industrial revolution have  
40 improved over the past few decades [Chen and Millero, 1979; Gruber et al., 1996]; [Sabine et  
41 al., 2008]; [Touratier and Goyet, 2004; 2009; Woosley et al., 2016]. As the concentration of  
42 anthropogenic carbon, C<sub>ant</sub>, cannot be distinguished from the natural background of DIC  
43 through total DIC measurements, these methods are based on the analysis of different  
44 chemical properties of the water column. Direct estimates of the anthropogenic CO<sub>2</sub>  
45 absorption in the sea surface layers are difficult owing to the large natural variability driven  
46 by physical and biological phenomena. [Bates et al., 2014] have extracted the trend from the  
47 large variability, based on analysis of a long time series (monthly or seasonal sampling). For  
48 the global surface ocean, [Lauvset et al., 2015] have used the Surface Ocean CO<sub>2</sub> Atlas  
49 (SOCAT) database [Bakker et al., 2014] combined with an interpolation method. Constraints  
50 on the Mediterranean Sea's storage of anthropogenic CO<sub>2</sub> are limited, as the data based  
51 approaches disagree by more than a factor of two [Huertas et al., 2009; Touratier and Goyet,  
52 2009].

53 A high frequency sampling of the seawater carbon chemistry at the air-water interface is a  
54 way to detect a possible trend in DIC related to the absorption of increasing atmospheric CO<sub>2</sub>  
55 concentration. In this paper we analyzed two three-year time series of hourly fugacity of CO<sub>2</sub>,  
56 fCO<sub>2</sub>, measured with autonomous CARIOCA sensors [Copin-Montégut et al., 2004; Merlivat  
57 and Brault, 1995] in 1995-1997 and 2013-2015, at two very close locations in the  
58 northwestern Mediterranean Sea (Fig. 1). Using measured fCO<sub>2</sub>, temperature, T, and salinity,  
59 S, we derived the other variables of the carbonate system (pH and DIC). The experimental  
60 setting is first described, and the recent data obtained over the 2013-2015 period are  
61 presented. Combined with the 1995-1997 measurements previously published [Hood and  
62 Merlivat, 2001], we estimated the decrease of pH and the increase of DIC. The results are  
63 compared with the respective contributions of the exchange with atmospheric CO<sub>2</sub> and with



64 recent estimates of the transport of anthropogenic carbon from the Atlantic Ocean over a 18  
65 years period.

66

## 67 2 Material and methods

### 68 2.1-The BOUSSOLE and DYFAMED sites

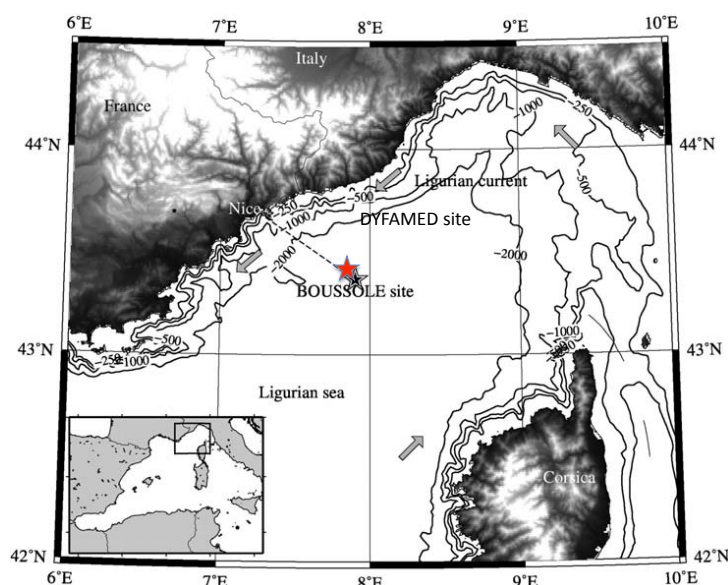


Fig. 1. The area of the northwestern Mediterranean Sea showing the southern coast of France, the island of Corsica, the main current branches (gray arrows), and the location of the DYFAMED site (red star) and the BOUSSOLE buoy (black star) in the Ligurian Sea.

69

70 Data collection was carried out at the BOUSSOLE site (43°22'N, 7°54'E) in 2013-2015  
71 [Antoine *et al.*, 2008; Antoine. and others, 2006] and at the DYFAMED site (43°25'N,  
72 7°52'E) in 1995-1997 [Marty *et al.*, 2002]. These sites are 3 nautical miles apart, both located  
73 in the Ligurian Sea, one of the basins of the northwestern Mediterranean Sea (Fig.1). The  
74 water depth is of ~2400 m. The prevailing ocean currents are usually weak ( $<20 \text{ cm s}^{-1}$ ),  
75 because these sites are in the central area of the cyclonic circulation that characterizes the  
76 Ligurian Sea [Millot, 1999]. The two sites are protected from coastal inputs by the Ligurian  
77 current. Monthly cruises are carried out at the same location.

78

### 79 2.2- Analytical methods

80 At DYFAMED,  $f\text{CO}_2$  measurements at 2m depth were provided by an anchored floating buoy  
81 fitted with a CARIOCA sensor. At BOUSSOLE, measurements were carried out from a



82 mooring normally dedicated to radiometry and optical measurements, and onto which two  
83 CARIOCA sensors were installed. They monitored  $f\text{CO}_2$  hourly at 3 and 10 meters depth  
84 (although only one of the two depths was equipped with a functional sensor at some periods);  
85 S and T were monitored at the same two depths using a Seabird SBE 37-SM MicroCat  
86 instrument. These CARIOCA sensors were adapted to work under pressure in the water  
87 column. They were swapped about every 6 months, with serviced and calibrated instruments  
88 replacing those having been previously deployed. The accuracy of  $f\text{CO}_2$  measurements using  
89 the spectrophotometric method with thymol blue is estimated at  $3 \mu\text{atm}$  [Copin-Montégut et  
90 al., 2004; Hood and Merlivat, 2001]. For *in situ* calibration of the newly designed  $f\text{CO}_2$   
91 sensors, seawater samples were taken at 5 and 10 meters depth during the monthly servicing  
92 cruises to the mooring and analyzed in terms of S, DIC, and total alkalinity, Alk. The samples  
93 were analyzed using potentiometric titration from the method developed by [Edmond, 1970]  
94 with a closed cell. For calibration, Certified Reference Materials (CRMs) provided by Prof.  
95 A. Dickson (Scripps Institution of Oceanography, San Diego, USA) were used. The accuracy  
96 is estimated at  $3 \mu\text{mol kg}^{-1}$  for both  $\text{TCO}_2$  and Alk.  $f\text{CO}_2$  is calculated using the dissociation  
97 constants of Mehrbach refitted by Dickson and Millero [Dickson and Millero, 1987;  
98 Mehrbach et al., 1973]. Its error is expected to be on the order of  $5 \mu\text{atm}$  [Millero, 2007] so  
99 that if the errors are fully random, the error on the mean of the 56 samples corresponding on  
100 the error on the absolute calibration of the sensor  $f\text{CO}_2$ , is  $0.7 \mu\text{atm}$ . In fact, the standard  
101 deviation of the difference between the  $f\text{CO}_2$  sensor data and  $f\text{CO}_2$  computed with the  
102 monthly discrete samples (Fig. 2b) is equal to  $4.4 \mu\text{atm}$ , very consistent with the expected  
103 error on individual estimate. Alk and S of the 56 samples taken at BOUSSOLE are linearly  
104 correlated according the following relationship :

$$105 \quad \text{Alk } (\mu\text{mol kg}^{-1}) = 87.647 \text{ S} - 785.5 \quad (1)$$

106 The standard deviation on predicted Alk is equal to  $4.4 \mu\text{mol kg}^{-1}$  ( $r^2=0.89$ ).

107

### 108 **3 Results**

#### 109 **3.1 The BOUSSOLE mooring (2013-2015) time series**

110 Temperature,  $f\text{CO}_2$  and  $f\text{CO}_2@13$  were measured from February 2013 to February 2016. All  
111 seasons were well represented, with missing data only in May-July 2013. For some periods,  
112 simultaneous measurements were made at 3 and 10 m depth (Fig. 2, a, b, c).

113

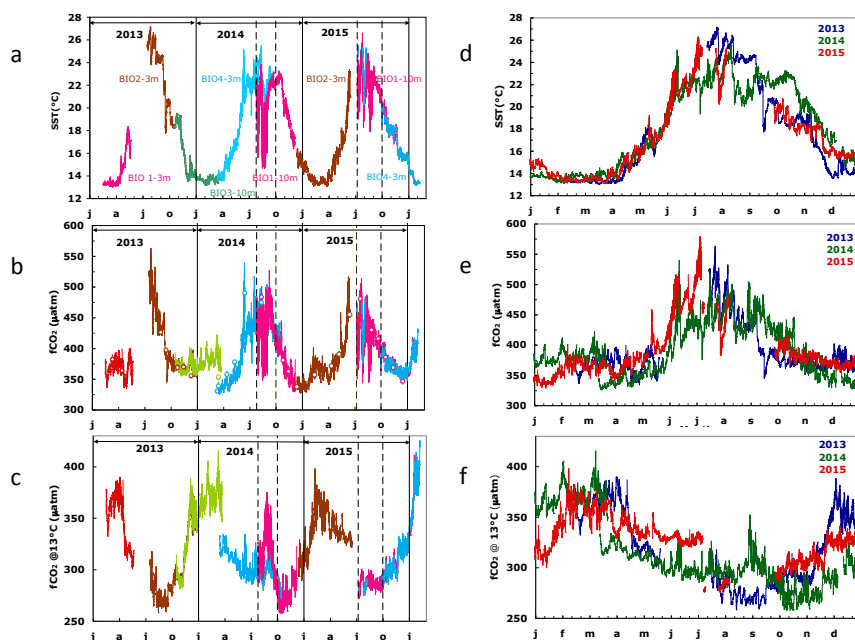


Fig.2. Interannual variability of CARIOCA data :a) T, b)  $f\text{CO}_2$ , c)  $f\text{CO}_2$  at  $13^\circ\text{C}$ . The dotted lines indicate the period strongly affected by stratification and internal waves (July, 26<sup>th</sup> to October 1<sup>st</sup>, 2014 and July, 8<sup>th</sup> to October 1<sup>st</sup>, 2015). On 2(b), the open circles correspond to  $f\text{CO}_2$  data derived from DIC and alkalinity measurements of samples taken at 5 and 10 meters. (d), (e), (f), seasonal variability.

114

115 The range of temperature (Fig. 2a) extends from  $13^\circ\text{C}$  in winter up to  $27^\circ\text{C}$  in summer,  
 116 followed by progressive cooling in fall. The coldest temperature,  $13^\circ\text{C}$ , results from the  
 117 winter vertical mixing with the deeper Levantine Intermediate Water, LIW, marked by  
 118 extrema in temperature and salinity [Copin-Montegut and Begovic, 2002]. Temperature  
 119 provides the main control of the seasonality of  $f\text{CO}_2$ , from  $350 \mu\text{atm}$  to more than  $550 \mu\text{atm}$   
 120 in summer 2013 (Fig. 2b). The fugacity of  $\text{CO}_2$  in seawater is a function of temperature, DIC,  
 121 alkalinity, and salinity. Among these, for the conditions encountered in the Mediterranean  
 122 sea, temperature and DIC have the strongest influences, whereas changes in alkalinity and  
 123 salinity have only minor effects [Takahashi et al., 1993]. By normalizing  $f\text{CO}_2$  to a constant  
 124 temperature, the thermodynamic effect can be removed and changes in  $f\text{CO}_2$  resulting from  
 125 changes in DIC can be more easily identified. Figure 2c shows the variability of  $f\text{CO}_2$   
 126 normalized to the constant temperature of  $13^\circ\text{C}$ , ( $f\text{CO}_2@13$ ), using the equation of  
 127 [Takahashi et al., 1993]. The underlying processes that govern the seasonal variability of  
 128  $f\text{CO}_2@13$  are successively winter mixing, biological activity, remineralization and deepening  
 129 of mixed layer in fall [Begovic and Copin-Montegut, 2002; Hood and Merlivat, 2001].  
 130 Biology accounts for the decay of  $f\text{CO}_2@13$  observed from March-April to late summer;



131 increase of surface  $f\text{CO}_2@13$  is associated with the deepening of the mixed layer in the fall or  
132 convection in winter as the vertical distribution of  $f\text{CO}_2@13$  at DYFAMED shows a  
133 maximum in the 50-150 m layer where a large remineralization of organic matter occurs, the  
134 productive layer being mostly between 0 and 40 m. The contribution of air-sea exchange is  
135 not significant. During summer 2014, large differences between measurements at 3 and  
136 10 meters were observed (Fig. 2, a, b, c between dashed lines). A detailed analysis of the  
137 temporal variability during that period underscores the role of inertial waves at the  
138 frequency of 17.4 hours that create the observed differences between the 2 depths of  
139 observations, the deeper waters being colder and enriched in  $f\text{CO}_2@13$ . T and  $f\text{CO}_2@13$   
140 variability is dominated by inertial waves. In particular, from 15<sup>th</sup> to 26<sup>th</sup> of August  
141 2014, the difference in T between the two depths is as large as 7.6°C, and 5.1°C on  
142 average. Likewise,  $f\text{CO}_2$  decreases on average by 32.7  $\mu\text{atm}$  leading to an increase of  
143  $f\text{CO}_2@13$  equal to 42.8  $\mu\text{atm}$ .

144 The 2013-2015 seasonal and inter-annual variability of T,  $f\text{CO}_2$  and  $f\text{CO}_2@13$  is  
145 illustrated on Fig. 2, d, e, f. The larger interannual changes in temperature (Fig.2, d) are  
146 observed during summer, both at 3m and 10m depth, while over February and March, a  
147 constant value of 13°C is observed as the result of vertical mixing with the LIW. A very  
148 large inter-annual variability of  $f\text{CO}_2@13$  is observed for  $T < 14^\circ\text{C}$  (Fig. 2,f). This is  
149 associated with the winter mixing at the mooring site, which is highly variable from year  
150 to year. Winter mixed-layer depth, MLD, varies between 30 and 200-300 m, at the top of  
151 the LIW. The variable depth of the winter vertical mixing causes the difference in  
152  $f\text{CO}_2@13$  as  $f\text{CO}_2$  increases with depth [Copin-Montegut and Begovic, 2002]. The  
153 deepening of MLD is driven by episodic and intense mixing processes characterized by a  
154 succession of events lasting several days, related to atmospheric forcing [Antoine et al.,  
155 2008] which lead to increase in  $f\text{CO}_2@13$ . Figure 2,e illustrates the solubility control of  
156 the variability of  $f\text{CO}_2$ , as  $f\text{CO}_2$  increases when T increases. Another cause of inter-  
157 annual variability of  $f\text{CO}_2$  for  $T \sim 14^\circ\text{C}$  is the timing of the spring increase of biological  
158 activity which differs by a month between years; for instance, it happened at the  
159 beginning of April in 2013,  $T \sim 15\text{-}16^\circ\text{C}$  and by mid March in 2014,  $T \sim 14^\circ\text{C}$ . Another  
160 cause is the deepening of the mixed layer due to the fall cooling which varies by a month  
161 between years.

162

163 **3.2 Decadal changes of hydrography**



164 **3.2.1** Sea surface temperature changes

165 Monthly mean values of temperature have been computed for the two three-year periods,  
166 1995-1997 and 2013-2015. In 1995-1997,  $f\text{CO}_2$  and T at 2m were measured with CARIOCA  
167 sensors installed on a buoy at DYFAMED [*Hood and Merlivat, 2001*]. The mean annual  
168 temperature of hourly CARIOCA data is equal to 18.21°C. For 2013-2015, temperature  
169 measurements made on the BOUSSOLE mooring at 3 and 10 meters have been used. For the  
170 April to September time interval, there are only data at 3m depth. In addition, temperature  
171 data measured half hourly at 0.7 m at a nearby meteorological buoy (43°23'N, 7°50'E)  
172 (<http://www.meteo.shom.fr/real-time/html/DYFAMED.html>) have been used (Fig.3d). Mean  
173 annual temperature are equal to 18.29°C and 17.97°C respectively, based on the  
174 meteorological buoy and the BOUSSOLE mooring data. The two sets of data differ  
175 essentially during July and August, with the temperatures at 3m being colder than at 0.7m,  
176 indicating a thermal gradient between the two depths during summer. Therefore, for 2013-  
177 2015, we select the mean annual value computed with the meteorological buoy, 18.29°C, as  
178 better representing the sea surface. This value is very close to 18.21°C computed for 1995-  
179 1997. Then, no significant change of SST is found between the 2 decades, with a mean value  
180 equal to 18.25°C.

181 **3.2.2** Sea surface salinity changes

182 The mean value of salinity computed from 56 samples taken at BOUSSOLE in 2013-2015 is  
183 equal to 38.19±0.14. In 1998-1999, ship measurements of surface salinity were made during  
184 monthly cruises at the DYFAMED site [*Copin-Montégut et al., 2004*]. The mean salinity of  
185 this set of 19 data is equal to 38.21±0.12. Thus, there is no significant salinity change  
186 between the two decades.

187

188 **3.3** Decadal changes of  $f\text{CO}_2@13$

189 **3.3.1** Time series of  $f\text{CO}_2@13$  in 1995-1997 and 2013-2015

190 The two time series of high frequency data were analyzed in order to quantify the change of  
191  $f\text{CO}_2@13$  at the sea surface two decades apart. To account for the interannual seasonal  
192 variability as well as irregular sampling, we performed an analysis of the change of  $f\text{CO}_2@13$   
193 as a function of SST (Fig. 3, a and b). For the 2013-2015 data set, we excluded summer data  
194 measured at 10 m depth as they were not representative of the surface mixed layer due to a  
195 strong stratification. Much larger  $f\text{CO}_2@13$  values are observed at low temperature than at  
196 high temperature, the decrease being similar for the two studied periods and strongly non  
197 linear. As described in section 3.1, large values at low temperature result from mixing with



198 enriched deep waters during winter and low values for 26°C-28°C temperatures occur at the  
 199 end of summer after biological drawdown of carbon. An increase of  $f\text{CO}_2@13$  between the 2  
 200 periods is clearly highlighted for the whole range of temperature. No interannual bias of the  
 201 observed data is displayed.

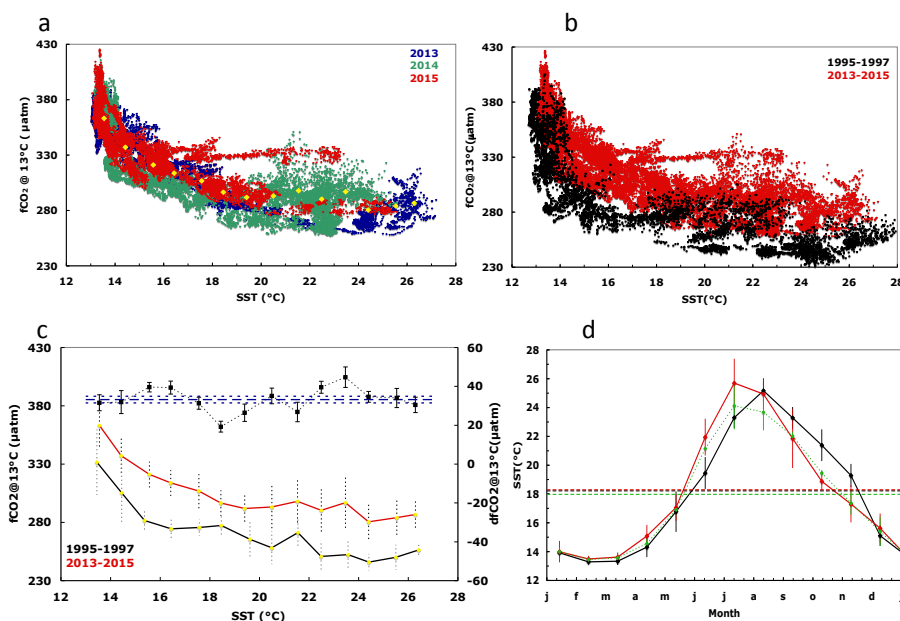


Fig.3. (a)  $f\text{CO}_2@13$  as a function of temperature for hourly data in 2013, 2014 and 2015 (b) as in (a) but for all hourly data in 1995-1997 (black) and in 2013-2015 (red) (c) As in (b), but for average values per 1°C interval (standard deviation as dotted line). The difference between the two periods is also displayed (dashed black curve; scale on the right axis). (d) Mean monthly sea surface temperature for 1993-1995 (black curve; CARIOCA sensors), 2013-2015 (green; CARIOCA sensors), 2013-2015 (red, meteorological buoy). Corresponding mean annual values are indicated by dotted lines.

202

203

### 204 3.3.2 Trend analysis and statistics

205 To quantify the change of  $f\text{CO}_2@13$  between the two data sets, we proceeded as follows: data  
 206 were binned by 1°C temperature intervals, thereby removing any potential seasonal  
 207 weighting, especially towards the 13-14°C winter months temperature. The measurements  
 208 made in this temperature interval represent about 25% of the total number of data for both  
 209 periods. For each of the fourteen 1°C step, the mean, standard deviation of hourly  $f\text{CO}_2@13$   
 210 measurements were computed (Table 1). For both data sets, a monotonous relationship  
 211 between  $f\text{CO}_2@13$  and T is observed with correlation coefficients respectively equal to -  
 212 0.861 and -0.857 (Fig. 3c). The increase of  $f\text{CO}_2@13$  between the two time series,  
 213  $df\text{CO}_2@13$ , was computed for each 1°C temperature interval. The mean value of  $df\text{CO}_2@13$





214 is equal to 33.17  $\mu\text{atm}$  with a standard error equal to 1.68 $\mu\text{atm}$ . It is interesting to note that  
 215  $\text{dfCO}_2@13$  is evenly distributed in the whole range of temperature (Fig. 3c), which  
 216 suggests that the processes which control the seasonal variation of  $\text{fCO}_2@13$  at the sea  
 217 surface have not changed over the 2 last decades at the exception of the  $\text{CO}_2$  air-sea flux .

Table 1

Time interval 1995-1997				Time interval 2013-2015				Temporal trend	
$T^1$	$\text{fCO}_2@13$	N	standard deviation	$T^1$	$\text{fCO}_2@13$	N	standard deviation	$\text{dfCO}_2@13$	standard error <sup>2</sup>
$^{\circ}\text{C}$	$\mu\text{atm}$		$\mu\text{atm}$	$^{\circ}\text{C}$	$\mu\text{atm}$		$\mu\text{atm}$	$\mu\text{atm}$	$\mu\text{atm}$
13.45	331.58	1212	28.09	13.55	363.14	6869	18.07	31.56	4.09
14.45	305.28	495	26.02	14.43	337.16	3270	16.65	31.87	5.91
15.37	281.54	447	9.62	15.57	321.10	3112	11.09	39.56	2.43
16.44	274.43	182	8.53	16.42	313.79	1818	11.09	39.36	3.35
17.58	275.54	190	7.04	17.56	306.83	1528	14.65	31.29	3.10
18.47	277.34	300	9.04	18.45	296.57	2621	10.95	19.23	2.76
19.62	265.43	342	15.58	19.41	291.84	1406	13.45	26.40	4.49
20.50	258.08	529	145	20.50	293.16	1135	18.21	35.08	4.01
21.56	271.15	239	12.98	21.54	297.96	1200	20.41	26.82	5.02
22.49	250.75	742	13.66	22.49	290.27	2385	18.57	39.52	3.08
23.57	252.22	320	13.00	23.47	296.92	747	21.77	44.70	5.28
24.41	245.85	506	7.08	24.40	280.44	959	14.82	34.59	2.81
25.50	250.06	215	10.77	25.53	284.05	456	14.81	33.99	4.95
26.42	256.29	279	6.24	26.29	286.71	249	11.23	30.42	3.94

1)The mean temperatures within each 1° step differ for the 2 periods as the distribution of individual measurements are not identical.

2) The daily scale is used to compute the standard error ( $n=N/24$ )

218

219

Table 1:

220 Distribution of temperature,  $\text{fCO}_2@13$ , and increase  $\text{dfCO}_2@13$  data binned by 1°C

221 temperature interval for the 2 periods 1995-1997 and 2013-2015 .

222

223 **3.4 Changes of seawater carbonate chemistry in surface waters**

224 We estimated the DIC and  $\text{pH}_T$  changes related to the increase of  $\text{fCO}_2@13$  measured at the  
 225 sea surface 18 years apart, assuming a mean salinity equal to 38.2, a mean alkalinity equal to  
 226 2562.3  $\mu\text{mol kg}^{-1}$  following equation (1), and a mean in situ temperature, T, equal to 18.25°C.

227 The dissociation constants of Mehrbach refitted by Dickson and Millero [Dickson and  
 228 Millero, 1987; Mehrbach et al., 1973] were used.  $\text{pH}$  is calculated on the seawater scale.

229 In the range of the  $\text{fCO}_2$  observations, DIC and  $\text{fCO}_2@T$  or  $\text{pH}_T$  and  $\text{fCO}_2@T$  are linearly  
 230 related with slopes respectively equal to 0.5982 (+/-0.0046)  $\mu\text{molkg}^{-1}/\mu\text{atm}$  ( $r^2=0.9993$ ) and -



231 0.0009 (+/-0.0002) pH<sub>T</sub> unit/μatm ( $r^2=0.9997$ ). We used these sensitivity factors to compute  
 232 the increase of DIC, dDIC, equal to 24.78±1.26 μmol kg<sup>-1</sup> (1.38±0.07 μmol kg<sup>-1</sup>yr<sup>-1</sup>) and  
 233 the decrease of pH<sub>T</sub>, dpH<sub>T</sub> equal to -0.0373±0.0019 pH<sub>T</sub> unit (-0.0021±0.0001 pH<sub>T</sub> unityr<sup>-1</sup>)  
 234 <sup>1</sup>) (Table 2).

Table 2

	d fCO <sub>2</sub> <sup>*</sup> @ 13°C μatm	d fCO <sub>2</sub> <sup>*</sup> @ T μatm	d DIC <sup>*</sup> μmolkg <sup>-1</sup>	d pH <sub>T</sub> <sup>*</sup> pH unit	dfCO <sub>2</sub> @T annual μatm yr <sup>-1</sup>	d DIC annual μmolkg <sup>-1</sup> yr <sup>-1</sup>	d pH <sub>T</sub> annual pH unit yr <sup>-1</sup>
sea surface	33.17 ±1.68	41.42 ±2.10	24.78 ±1.26	-0.0373 ±0.0019	2.30 ±0.12	1.38 ±0.07	-0.0021 ±0.0001
atmosphere Lampedusa data		34.9 ±0.9	**20.88±/ 0.53		1.94 ±0.05		
dfCO <sub>2</sub> @T <sub>air</sub> /dfCO <sub>2</sub> @T <sub>sea</sub>		0.84 ±0.05					

T<sub>i</sub> mean annual temperature equal to 18.25°C

\* Change from 1993-1995 to 2013-2015

\*\* dDIC<sub>ant</sub>

235

236

Table 2

237 Seasonally detrended long term and annual trends of seawater carbonate chemistry and  
 238 atmosphere composition.

239

### 240 3.5 Changes in atmospheric and seawater fCO<sub>2</sub>

241 The increase of atmospheric fCO<sub>2</sub> from 1995-1997 to 2013-2015 was computed from the  
 242 monthly atmospheric xCO<sub>2</sub> concentrations measured at the Lampedusa Island station (Italy)  
 243 (35°31'N, 12°37'E) (<http://ds.data.jma.go.jp/gmd/wdcdgg/>). Considering a mean annual in situ  
 244 temperature equal to 18.25°C and an atmospheric pressure equal to 1 atm, we derived a mean  
 245 atmospheric fCO<sub>2</sub> equal to 355.2±0.6 μatm and 390.1±0.7 μatm for 1995-1997 and 2013-  
 246 2015, that is an increase equal to 34.9±0.9 μatm (Table 2). At this temperature, the change  
 247 of fCO<sub>2</sub> at the sea surface is equal to 41.4±2.1 μatm. Thus the contribution of the increase in  
 248 atmospheric CO<sub>2</sub> is responsible for 84±5 % of the increase of fCO<sub>2</sub> measured in the surface  
 249 waters. Assuming the same salinity and alkalinity as previously, the corresponding amount of  
 250 anthropogenic carbon taken up from the atmosphere in order to maintain a chemical  
 251 equilibrium at the sea surface would be equal to 20.88±0.53 μmol kg<sup>-1</sup> (Table 2).

252

## 253 4 Discussion



#### 254 4.1 fCO<sub>2</sub> at the air-sea interface

255 We have computed that 84% of the increase of fCO<sub>2</sub> <sub>sea</sub> in the northwestern Mediterranean,  
256 two decades apart, comes from the atmosphere. One implicit assumption is that any change in  
257 atmospheric fCO<sub>2</sub> immediately transfers as a change in the surface ocean fCO<sub>2</sub>. In agreement  
258 with the circulation pattern of the basin [Millot, 1999], this increase of surface fCO<sub>2</sub> could  
259 follow two routes: in situ chemical equilibrium at the air-sea interface or winter mixing with  
260 surface waters of Atlantic origin, relatively enriched in anthropogenic carbon. Keeping in  
261 mind that the deep-water renewal time is estimated to be 20-40 years in the western basin, and  
262 given that the atmospheric increase was slower 20-40 years ago, our estimate of the  
263 atmospheric contribution to the ocean trend is likely an upper bound.

264 The mean values of fCO<sub>2</sub> computed at the mean annual SST, 18.25°, computed with all the  
265 individual hourly fCO<sub>2</sub> measurements in 1995-1997 and 2013-2015 are respectively equal to  
266 352.3 μatm and 400.2 μatm, while the corresponding atmospheric values are 355.2 μatm and  
267 390.1 μatm respectively. The close values of fCO<sub>2</sub> <sub>sea</sub> and fCO<sub>2</sub> <sub>air</sub> in 1995-1997 indicate an  
268 near-balanced air to sea CO<sub>2</sub> flux on an annual time scale as previously shown by [Hood and  
269 Merlivat, 2001]. For the 2013-2015 period, a positive annual average air-sea disequilibrium is  
270 observed leading to a medium source for the atmospheric CO<sub>2</sub>. This is consistent as the result  
271 of the supplementary contribution of Atlantic waters anthropogenic carbon (+6.5 μatm)  
272 (Table 2) in this region of the Mediterranean sea.

273

#### 274 4.2 Time change of surface alkalinity?

275 In the range of salinity of the BOUSSOLE samples, 37.9 to 38.5 psu, the alkalinity values  
276 computed with Eq (1) are larger than those predicted by the [Copin-Montegut and Begovic,  
277 2002] relationship established for the DYFAMED site, with a mean difference equal to 10+/-  
278 2 μmol kg<sup>-1</sup>. In both cases alkalinity measurements were made with a potentiometric method  
279 using certified reference material supplied by AG Dickson for calibration.

280 It is difficult to identify the cause for a possible change of alkalinity between the 2 periods, 18  
281 years apart, while no salinity change has been observed. At a coastal site 50 km away from  
282 DYFAMED, [Kapsenberg et al., 2017] have measured an increase of alkalinity unrelated to  
283 salinity over the period from 2007 to 2015. They attribute it to changes in freshwater inputs  
284 from land. However, based on data from Coppola et al., [2016], alkalinity in the upper 50m at  
285 DYFAMED did not change significantly from 2007 through 2014 (3.204 μmol kg<sup>-1</sup>,  
286 P=0,0794, r<sup>2</sup>=0.08). Thus, we cannot conclude on whether the difference observed at  
287 DYFAMED/BOUSSOLE between the two periods is real or an artifact of measurement



288 techniques. However, as a sensitivity test, if we compute the expected changes of DIC and pH  
289 from 1995-1997 to 2013-2015 for a mean alkalinity increase of  $10 \mu\text{mol kg}^{-1}$ , we get annual  
290 changes,  $d\text{DIC}=+0.46 \mu\text{mol kg}^{-1}\text{yr}^{-1}$  and  $d\text{pH}=-0.0001 \text{ pH unit yr}^{-1}$ . It is thus interesting to  
291 notice that such a change in alkalinity does not impact significantly the decrease of pH shown  
292 in Table 2.

293

#### 294 4.3 Anthropogenic carbon storage in surface waters

295 The increase of sea surface DIC from 1995-1997 to 2013-2015 due to the uptake of  
296 atmospheric  $\text{CO}_2$ , referred here as anthropogenic DIC ( $d\text{DIC}_{\text{ant}}$ ), is equal to  $24.78\pm 1.26$   
297  $\mu\text{mol kg}^{-1}$  (Table 2). ( $d\text{DIC}_{\text{ant}}$ ) predicted solely from chemical equilibrium of the sea surface  
298 with the atmosphere is equal to  $20.88\pm 0.53 \mu\text{mol kg}^{-1}$ . The ratio of these two terms is equal  
299 to  $0.84\pm 0.05$ . This calls upon an additional contribution to the local  $\text{CO}_2$  air-sea exchange.  
300 As a result of a monitoring program in the Strait of Gibraltar, [Huertas *et al.*, 2009] calculated  
301 a net flux of  $C_{\text{ant}}$  from the Atlantic towards the Mediterranean basin. [Schneider *et al.*, 2010],  
302 using the transit time distribution method applied to a dataset from a cruise in the  
303 Mediterranean Sea in 2001, estimated that the input of  $C_{\text{ant}}$  through the Strait of Gibraltar  
304 from 1850 to 2001 accounts for almost 10% of the total  $C_{\text{ant}}$  inventory of the Mediterranean  
305 Sea, which means that  $\sim 90\%$  must have been taken up directly from the atmosphere. Based on  
306 a high-resolution regional model, [Palmiéri *et al.*, 2015] computed the anthropogenic carbon  
307 storage in the Mediterranean basin. They concluded that 75% of the total storage of  $C_{\text{ant}}$  in the  
308 whole basin comes from the atmosphere and 25% from net transport from the Atlantic across  
309 the Strait of Gibraltar. [Huertas *et al.*, 2009] and [Schneider *et al.*, 2010] report  $\text{DIC}_{\text{ant}}$  surface  
310 concentrations respectively equal to  $65\text{--}70 \mu\text{mol kg}^{-1}$  at the strait of Gibraltar in the years  
311 2005-2007 and close to  $65 \mu\text{mol kg}^{-1}$  in the western basin in 2001. We extrapolate these  
312 figures to the year 2014, assuming a mean increase rate of DIC equal to  $1.38 \mu\text{mol kg}^{-1}\text{yr}^{-1}$  as  
313 previously computed (Table 2). Taking into account the increase of  $\text{DIC}_{\text{ant}}$  equal to  $24.8 \mu\text{mol}$   
314  $\text{kg}^{-1}$  between 1995-1997 and 2013-2015, we estimate that the contribution of the change of  
315  $\text{DIC}_{\text{ant}}$  over the last 18 years represents  $\sim 30\%$  of the total change since the beginning of the  
316 industrial period ( $t > \sim 1800$ ).

317

#### 318 4.4 The signal of acidification

319 The annual decrease of  $\text{pH}_T$  calculated between 1995-1997 and 2013-2015 is equal to -  
320  $0.0021\pm 0.0001$ . At the DYFAMED site, at 10 m depth, [Marcellin Yao *et al.*, 2016] studied  
321 the time variability of pH over 1995-2011, based on measurements of T, S, Alk and DIC



322 sampled approximately once a month. They computed a mean annual decrease of  $-0.003 \pm$   
323  $0.001$  pH units on the seawater scale that is not significantly different from our estimate.  
324 [Bates *et al.*, 2014] examined changes in surface seawater CO<sub>2</sub>-carbonate chemistry at the  
325 locations of seven ocean CO<sub>2</sub> time series that have been gathering sustained observations  
326 from 15 to 30 years with monthly or seasonal sampling. The range of decreasing trends of pH  
327 extends from  $-0.0026 \pm 0.0006$  unit yr<sup>-1</sup> at the Irminger Sea time series site to  $-0.0014 \pm$   
328  $0.0005$  unit yr<sup>-1</sup> at the Iceland Sea time series. For the global surface ocean, [Lauvset *et al.*,  
329 2015] have reported a mean rate of decrease of  $-0.0018 \pm 0.0004$  for 1991-2011. The decrease  
330 of pH computed here at DYFAMED is in the upper range of values compared to other time  
331 series. The Mediterranean Sea is actually able to absorb more anthropogenic CO<sub>2</sub> per unit  
332 area, first because of its higher total alkalinity that leads to a greater chemical capacity to take  
333 up anthropogenic CO<sub>2</sub> and, second, because deep waters are ventilated on relatively short  
334 timescales (30-40 years in the western basin), which allows deeper penetration of  
335 anthropogenic tracers [Schneider *et al.*, 2010], [Palmiéri *et al.*, 2015]. The lowering effect of  
336 high alkalinity on the Revelle factor implies a relatively high uptake capacity for  
337 anthropogenic carbon, C<sub>ant.</sub>. However, this barely modifies the pH trend for a given change of  
338 fCO<sub>2</sub>.

339

## 340 5 Conclusion

341 High-frequency ocean fCO<sub>2</sub> measurements made by CARIOCA sensors were sufficient to  
342 estimate trends in fCO<sub>2</sub>, DIC and pH over a period of two decades, notwithstanding a  
343 considerable short-time variability of these properties at the sea surface. We have estimated a  
344 large change of sea surface carbonate chemistry and a decrease of pH due to uptake of  
345 anthropogenic CO<sub>2</sub>. In addition to providing first in situ estimates of the change expected  
346 from chemical equilibrium with atmospheric CO<sub>2</sub>, our results support modeling work and  
347 analysis of vertical profiles measurements that suggest that the Atlantic Ocean contributes as  
348 a source of 15% of the anthropogenic carbon for the basin.

349

350 *Data availability:* Time series data from Dyfamed (1995-1997) are available in the SOCAT v3  
351 database. Boussole data (2013-2015) will be available in SOCAT v6.

352

## 353 Acknowledgments

354 Seawater samples were analyzed for DIC and Alk by the SNAPO-CO<sub>2</sub> at LOCEAN in Paris.  
355 The CO<sub>2</sub>Sys toolbox of [Pierrot *et al.*, 2006] has been used for the calculations of DIC and



356 pH. The adaptation of CARIOCA sensors to high pressure has been supported by the BIO-  
357 optics and CARbon EXperiment (BIOCAREX) project, funded by the Agence Nationale de la  
358 Recherche (ANR,Paris). We are grateful for helpful comments from Gilles Reverdin on the  
359 manuscript.

360

### 361 **References**

362 Antoine, D., F. d'Ortenzio, S. B. Hooker, G. Bécu, B. Gentili, D. Tailliez, and A. J. Scott  
363 (2008), Assessment of uncertainty in the ocean reflectance determined by three satellite  
364 ocean color sensors (MERIS, SeaWiFS and MODIS-A) at an offshore site in the  
365 Mediterranean Sea (BOUSSOLE project), *Journal of Geophysical Research*, 113(C7).

366 Antoine., and others (2006), BOUSSOLE: A Joint CNRS-INSU,ESA, CNES and NASA ocean  
367 color calibration and validation activity., *NASA Tech. Memo. 2006-214147*.

368 Bakker, D. C. E., et al. (2014), An update to the Surface Ocean CO<sub>2</sub> Atlas  
369 (SOCAT version 2), *Earth Syst. Sci. Data*, 6(1), 69-90.

370 Bates, N., Y. Astor, M. Church, K. Currie, J. Dore, M. Gonaález-Dávila, L. Lorenzoni, F.  
371 Muller-Karger, J. Olafsson, and M. Santa-Casiano (2014), A Time-Series View of Changing  
372 Ocean Chemistry Due to Ocean Uptake of Anthropogenic CO<sub>2</sub> and Ocean Acidification,  
373 *Oceanography*, 27(1), 126-141.

374 Begovic , M., and C. Copin-Montégut (2002), Processes controlling annual variations in  
375 the partial pressure of fCO<sub>2</sub> in surface waters of the central northwestern  
376 Mediterranean sea (Dyfamed site), *Deep-Sea Research II*, 49, 2031-2047.

377 Chen, G. T., and F. J. Millero (1979), Gradual increase of oceanic CO<sub>2</sub>, *Nature*, 277, 205-  
378 206.

379 Copin-Montégut, C., and M. Begovic (2002), Distributions of carbonate properties and  
380 oxygen along the water column (0–2000 m) in the central part of the NW Mediterranean  
381 Sea (Dyfamed site): influence of winter vertical mixing on air-sea CO<sub>2</sub> and O<sub>2</sub>  
382 exchanges, *Deep-Sea Research II* 49, 2049-2066.

383 Copin-Montégut, C., M. Bégovic, and L. Merlivat (2004), Variability of the partial pressure  
384 of CO<sub>2</sub> on diel to annual time scales in the Northwestern Mediterranean Sea, *Mar Chem*,  
385 85(3-4), 169-189.

386 Coppola, L., E. Diamond Riquier, and T. Carval (2016), Dyfamed observatory data,  
387 *SEANOE*.



- 388 Dickson, A. G., and F. J. Millero (1987), A comparison of the equilibrium constants for the  
389 dissociation of carbonic acid in seawater media, *Deep Sea Research Part A.*  
390 *Oceanographic Research Papers*, 34(10), 1733-1743.
- 391 Edmond, J. M. (1970), High precision determination of titration alkalinity and total  
392 carbon dioxide content of seawater by potentiometric titration, *Deep Sea research* 17(4),  
393 737-750.
- 394 Gattuso, J.-P., and L. Hansson (2011), Ocean Acidification, *Oxford University Press*, 352  
395 pp.
- 396 Gruber, N., J. L. Sarmiento, and T. F. Stocker (1996), An improved method for detecting  
397 anthropogenic CO<sub>2</sub> in the oceans, *Global Biogeochem Cy*, 10, 809-837.
- 398 Hood, E. M., and L. Merlivat (2001), Annual and interannual variations of fCO<sub>2</sub> in the  
399 northwestern Mediterranean Sea: Results from hourly measurements made by CARIOCA  
400 buoys, 1995-1997, *J Mar Res*, 59, 113-131.
- 401 Huertas, I. E., A. F. Ríos, J. García-Lafuente, A. Makaoui, S. ` Rodríguez-Gálvez, A. Sánchez-  
402 Román, A. Orbi, J. Ruiz, and F. F. and Pérez (2009), Anthropogenic and natural CO<sub>2</sub>  
403 exchange through the Strait of Gibraltar, *Biogeosciences*, 6, 647-662.
- 404 Kapsenberg, L., S. Alliouane, F. Gazeau, L. Mousseau, and J.-P. Gattuso (2017), Coastal  
405 ocean acidification and increasing total alkalinity in the northwestern Mediterranean  
406 Sea, *Ocean Science*, 13(3), 411-426.
- 407 Lauvset, S. K., N. Gruber, P. Landschützer, A. Olsen, and J. Tjiputra (2015), Trends and  
408 drivers in global surface ocean pH over the past 3 decades, *Biogeosciences*, 12(5), 1285-  
409 1298.
- 410 Marcellin Yao, K., O. Marcou, C. Goyet, V. Guglielmi, F. Touratier, and J.-P. Savy (2016),  
411 Time variability of the north-western Mediterranean Sea pH over 1995-2011, *Marine*  
412 *Environmental Research*, 116, 51-60.
- 413 Marty, J. C., J. Chiaverini, M. Pizay, D.,, and B. Avril (2002), Seasonal and interannual  
414 dynamics of nutrients and phytoplankton pigments in the western Mediterranean Sea at  
415 the DYFAMED time-series station (1991-1999), *Deep-Sea Research II*, 49, 1965-1985.
- 416 Mehrbach, C., C. H. Culberson, J. E. Hawley, and R. M. Pytkowicx (1973), Measurement of  
417 the apparent dissociation constants of carbonic acid in seawater at atmospheric  
418 pressure, *Limnol Oceanogr*, 18(6), 897-907.
- 419 Merlivat, L., and P. Brault (1995), CARIOCA BUOY: Carbon Dioxide Monitor, *Sea*  
420 *Technol*(October), 23-30.



- 421 Millero, F. J. (2007), The marine inorganic carbon cycle, *Chemical reviews*, 107(2), 308-  
422 341.
- 423 Millot (1999), Circulation in the Western Mediterranean Sea, *Journal of Marine Systems*,  
424 20, 423–442.
- 425 Palmiéri, J., J. C. Orr, J. C. Dutay, K. Béranger, A. Schneider, J. Beuvier, and S. Somot  
426 (2015), Simulated anthropogenic CO<sub>2</sub> storage and acidification of the Mediterranean  
427 Sea, *Biogeosciences*, 12(3), 781-802.
- 428 Pierrot, D., E. Lewis, and D. W. R. Wallace (2006), MS excel program developed for CO<sub>2</sub>  
429 system calculations, *In: Carbon Dioxide Information Analysis Center (ed.O.R.N.L.).*  
430 *US.Department of Energy, Oak Ridge, TN.*
- 431 Sabine, C. L., R. A. Feely, F. J. Millero, A. G. Dickson, C. Langdon, S. Mecking, and D. Greeley  
432 (2008), Decadal changes in Pacific carbon, *J.Geophys.Res.*, 113(C07021).
- 433 Schneider, A., T. Tanhua, A. Körtzinger, and D. W. R. Wallace (2010), High anthropogenic  
434 carbon content in the eastern Mediterranean, *Journal of Geophysical Research*, 115(C12).
- 435 Takahashi , T., J. Olafson, J. G. Goddard, D. W. Chipman , and G. Sutherland (1993),  
436 Seasonal variations of CO<sub>2</sub> and nutrients in the high-latitude surface oceans:a  
437 comparative study, *Global Biogeochem Cy*, 7(4), 843-878.
- 438 Touratier, F., and C. Goyet (2004), Applying the new TrOCA approach to assess the  
439 distribution of anthropogenic CO<sub>2</sub> in the Atlantic Ocean, *Journal of Marine Systems*, 46(1-  
440 4), 181-197.
- 441 Touratier, F., and C. Goyet (2009), Decadal evolution of anthropogenic CO<sub>2</sub> in the  
442 northwestern Mediterranean Sea from the mid-1990s to the mid-2000s, *Deep Sea*  
443 *Research Part I: Oceanographic Research Papers*, 56(10), 1708-1716.
- 444 Woosley, R. J., F. J. Millero, and R. Wanninkhof (2016), Rapid anthropogenic changes in  
445 CO<sub>2</sub>and pH in the Atlantic Ocean: 2003-2014, *Global Biogeochem Cy*, 30(1), 70-90.
- 446
- 447
- 448





448

## Figure caption and tables

449

450 Figure 1. The area of the northwestern Mediterranean Sea showing the southern coast of  
451 France, the Island of Corsica, the main current branches (gray arrows), and the location of the  
452 DYFAMED site (43°25'N, 7°52'E, red star) and the BOUSSOLE buoy (43°22'N, 7°54'E,  
453 black star) in the Ligurian Sea.

454

455 Figure 2. Interannual variability of CARIOCA data: a) T, b)  $f\text{CO}_2$ , c)  $f\text{CO}_2@13$  The dotted  
456 lines indicate the period strongly affected by stratification and internal waves (July, 26<sup>th</sup> to  
457 October 1<sup>st</sup>, 2014 and July, 8<sup>th</sup> to October 1<sup>st</sup>, 2015). On 2(b), the open circles correspond to  
458  $f\text{CO}_2$  data derived from DIC and alkalinity measurements of samples taken at 5 and 10 meters.  
459 (d), (e), (f), seasonal variability. Note that the color code on (d), (e), (f) is different from (a),  
460 (b), (c).

461

462 Figure 3. (a)  $f\text{CO}_2@13$  as a function of temperature for hourly data in 2013, 2014 and 2015  
463 (b) as in (a) but for all hourly data in 1995-1997 (black) and in 2013-2015 (red) (c) As in (b),  
464 but for average values per 1°C interval (standard deviation as dotted line). The difference  
465 between the two periods is also displayed (dashed black curve; scale on the right axis). (d)  
466 Mean monthly sea surface temperature for 1993-1995 (black curve; CARIOCA sensors),  
467 2013-2015 (green; CARIOCA sensors), 2013-2015 (red, meteorological buoy).  
468 Corresponding mean annual values are indicated by dotted lines.

469

470 Table 1:

471 Distribution of temperature,  $f\text{CO}_2@13$ , and increase  $df\text{CO}_2@13$  data binned by 1°C  
472 temperature interval for the 2 periods 1995-1997 and 2013-2015 .

473

474 Table 2

475 Seasonally detrended long term and annual trends of seawater carbonate chemistry and  
476 atmosphere composition.

477